Supporting Information

Fluoride-ion shuttle battery with high volumetric energy density

Hiroyuki Nakano, Toshiyuki Matsunaga, Takuya Mori, Koji Nakanishi, Yoshiyuki Morita, Kazuto Ide, Ken-ichi Okazaki, Yuki Orikasa, Taketoshi Minato, Kentaro Yamamoto, Zempachi Ogumi, and Yoshiharu Uchimoto*

Contents

Table S1. Thermodynamically expected fluorination–defluorination potentials of several materials and calculated cell voltages and one-third of theoretical energy densities of several combinations of cathode and anode.

Material		Potential V vs. $Pb\|PbF_2$		Theoretical voltage V	One third of volumetric energy density Wh/L
Cathode	Anode	Cathode	Anode		
Ag	CaF_2	1.26	-2.85	4.11	1238
Ag	BaF_2	1.26	-2.80	4.06	885
Ag	MgF_2	1.26	-2.35	3.61	1294
Ag	LaF_3	1.26	-2.41	3.67	900
Ag	CeF_3	1.26	-2.37	3.63	916
Ag	AlF_3	1.26	-1.72	2.99	867
Cu	CaF_2	0.65	-2.85	3.49	1973
Cu	BaF_2	0.65	-2.80	3.44	1432
Cu	MgF_2	0.65	-2.35	2.99	1988
Cu	LaF_3	0.65	-2.41	3.05	1445
Cu	CeF_3	0.65	-2.37	3.01	1465
Cu	AlF_3	0.65	-1.72	2.37	1319
Co	CaF_2	0.64	-2.85	3.49	2715
Co	BaF_2	0.64	-2.80	3.44	2014
Co	MgF_2	0.64	-2.35	2.99	2697
Co	LaF_3	0.64	-2.41	3.05	2063
Co	CeF_3	0.64	-2.37	3.01	2089
Co	AlF_3	0.64	-1.72	2.37	1868
Sb	CaF_2	0.26	-2.85	3.11	1611
Sb	BaF_2	0.26	-2.80	3.06	1300
Sb	MgF_2	0.26	-2.35	2.61	1488
Sb	LaF_3	0.26	-2.41	2.67	1399
Sb	CeF_3	0.26	-2.37	2.63	1406
Sb	AlF_3	0.26	-1.72	1.99	1171
Bi	CaF_2	0.30	-2.85	3.15	1492
Bi	BaF_2	0.30	-2.80	3.10	1223
Bi	MgF_2	0.30	-2.35	2.65	1369
Bi	LaF_3	0.30	-2.41	2.71	1335
Bi	CeF_3	0.30	-2.37	2.67	1340
Bi	AlF_3	0.30	-1.72	2.02	1114
Ni	CaF_2	0.07	-2.85	2.92	1675
Ni	BaF_2	0.07	-2.80	2.86	1206
Ni	MgF_2	0.07	-2.35	2.42	1636
Ni	LaF_3	0.07	-2.41	2.47	1182
Ni	CeF_3	0.07	-2.37	2.44	1196
Ni	AlF_3	0.07	-1.72	1.79	1009
Pb	CaF_2	0.00	-2.85	2.85	1190
Pb	BaF_2	0.00	-2.80	2.80	924
Pb	MgF_2	0.00	-2.35	2.35	1103
Pb	LaF_3	0.00	-2.41	2.41	952
Pb	CeF_3	0.00	-2.37	2.37	958
Pb	AlF_3	0.00	-1.72	1.72	780
Fe	CaF_2	-0.16	-2.85	2.69	2050
Fe	BaF_2	-0.16	-2.80	2.64	1521
Fe	MgF_2	-0.16	-2.35	2.19	1928
Fe	LaF_3	-0.16	-2.41	2.25	1502
Fe	CeF_3	-0.16	-2.37	2.21	1514
Fe	AlF_3	-0.16	-1.72	1.56	1218

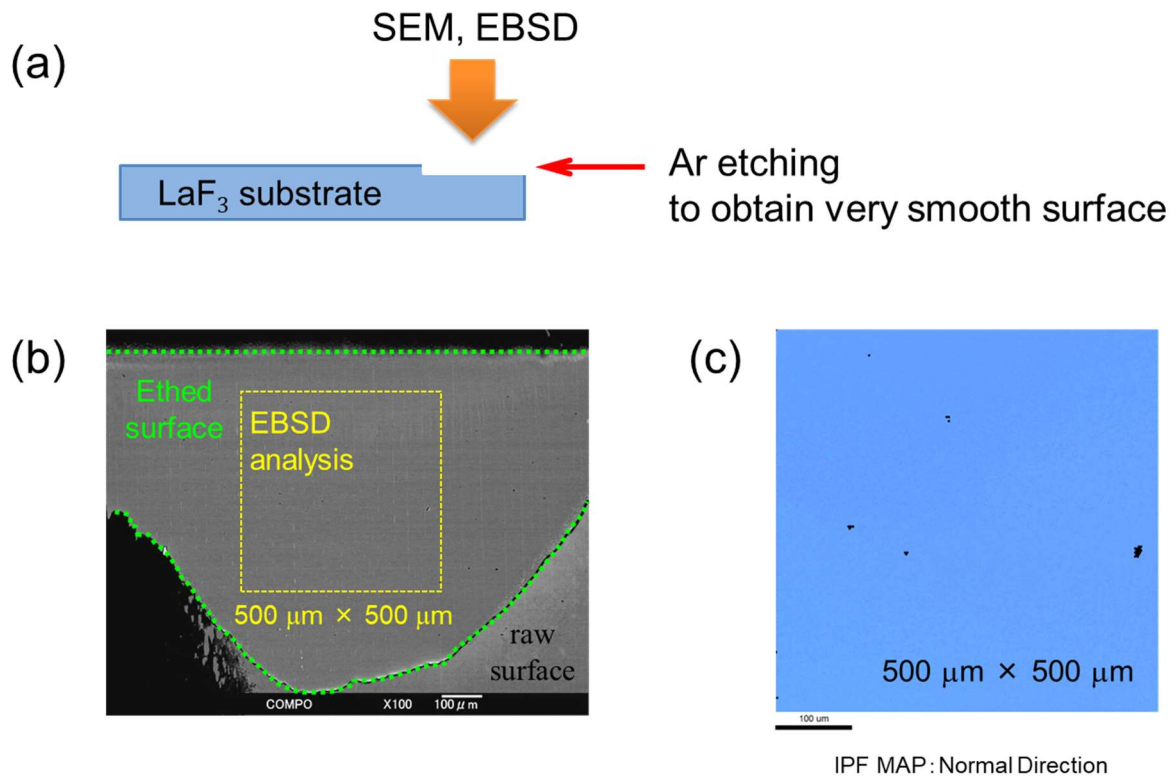

Figure S1. a) Illustration of the pre-treatment of the LaF_3 substrate for EBSD analysis. The raw LaF_3 surface was etched by Ar for obtaining a very smooth surface. b) SEM image of the pre-treated LaF_3 surface. The etched surface and EBSD analysis area are indicated by green and yellow, respectively. c) Crystal orientation mapping analysed by EBSD. Because there is no grain boundary of the LaF_3 substrate, the crystal orientation map was given by only one colour in a relatively wide area of 500 μm^2. This indicates that the LaF_3 substrate used in this study is a single crystal.

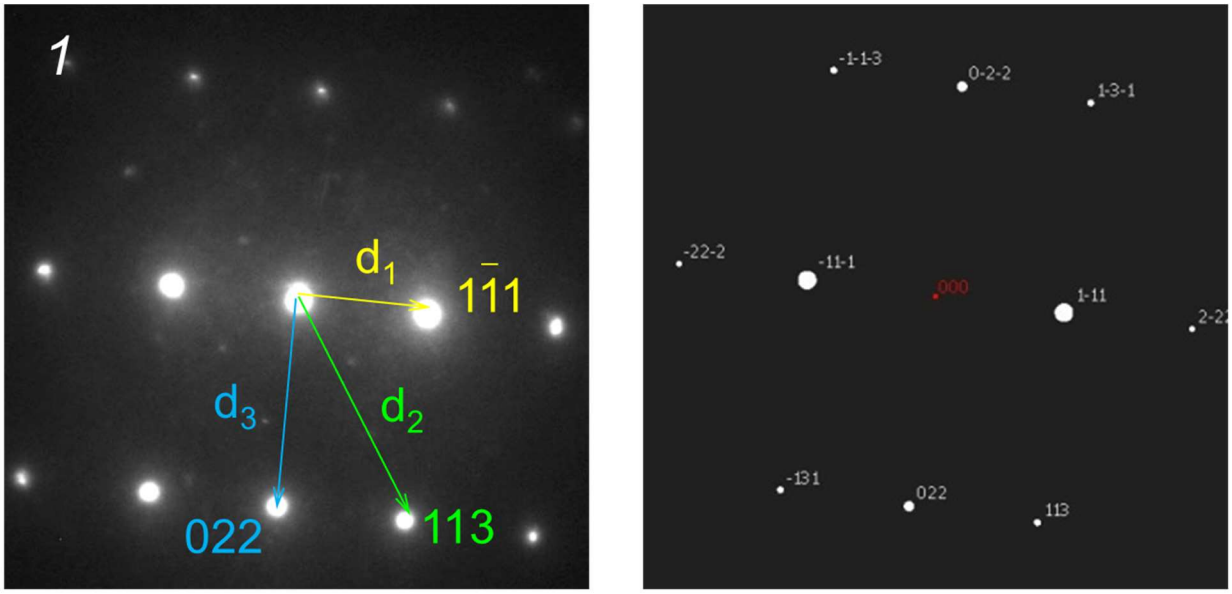

Material	Cu
Zone axis	[2 1 $\bar{1}$]
Crystal system	Cubic
Space group	$Fm\bar{3}m$
	a = 0.361 nm

d-spacing			
Experimental / nm		Simulated / nm	
(d_1)	0.201	($d_{1\text{-}11}$)	0.2087
(d_2)	0.110	(d_{113})	0.1090
(d_3)	0.130	(d_{022})	0.1278

Figure S2. Experimental (upper left) and simulated (upper right) ED patterns collected from cross section of Cu half-cells with various charge states. Miller indexes are also shown in the simulated ED pattern. Italic numbers shown in the experimental ED pattern indicate the analysed points or areas as shown in Figure 3 in the text. The assumed crystal structure for simulation is shown in the lower right. Three sets of d-spacing values calculated from experimental ED pattern and determined by simulation are shown in lower left. All sets of d-spacing values were almost identical, indicating that the assumed crystal structure is true.

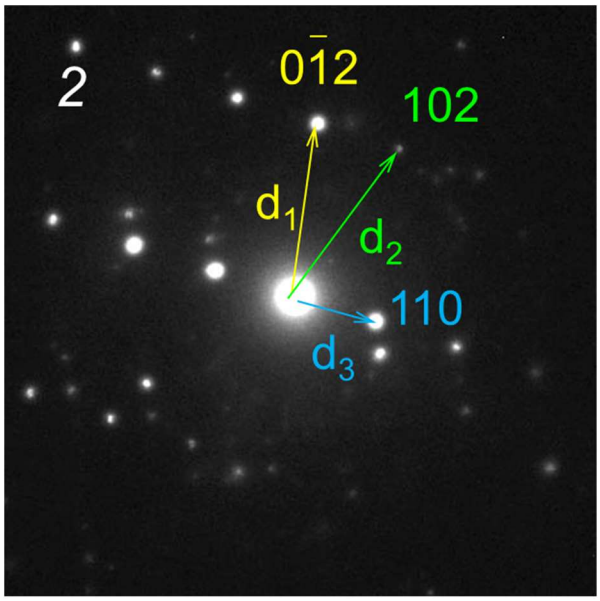

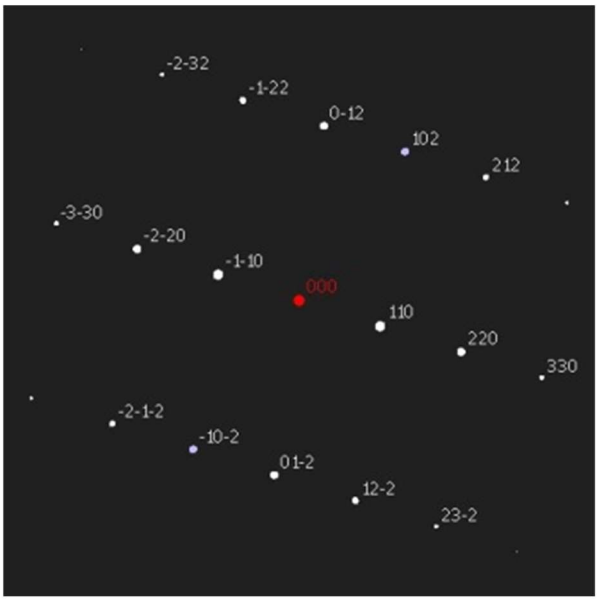

Material	CuF_2
Zone axis	$[2\ \bar{2}\ \bar{1}]$
Crystal system	monoclinic
Space group	$P\,2_1/c$
	$a = 0.459$ nm
	$b = 0.454$ nm
	$c = 0.332$ nm
	$\beta = 96.67°$

d-spacing			
Experimental / nm		Simulated / nm	
(d_1)	0.156	($d_{0\text{-}12}$)	0.1550
(d_2)	0.150	(d_{102})	0.1496
(d_3)	0.323	(d_{110})	0.3217

Figure S2. continued

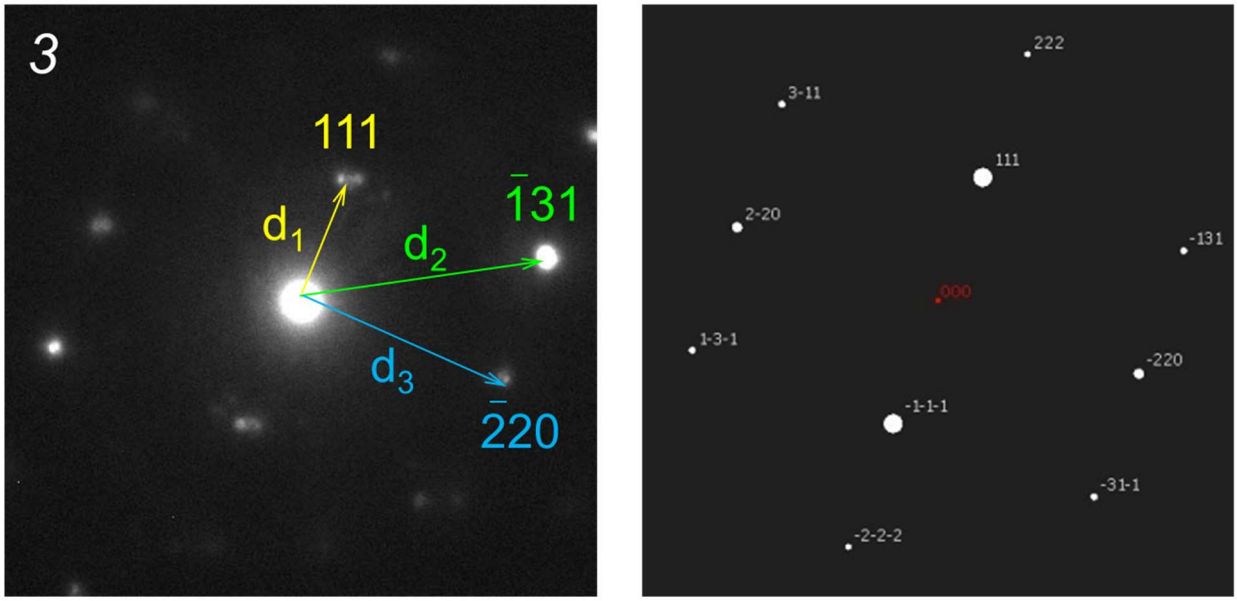

Material	Cu
Zone axis	[1 1 $\bar{2}$]
Crystal system	Cubic
Space group	$Fm\bar{3}m$
	a = 0.361 nm

d-spacing	
Experimental / nm	Simulated / nm
(d_1) 0.208	(d_{111}) 0.2087
(d_2) 0.109	(d_{-131}) 0.1090
(d_3) 0.125	(d_{-220}) 0.1278

Figure S2. continued

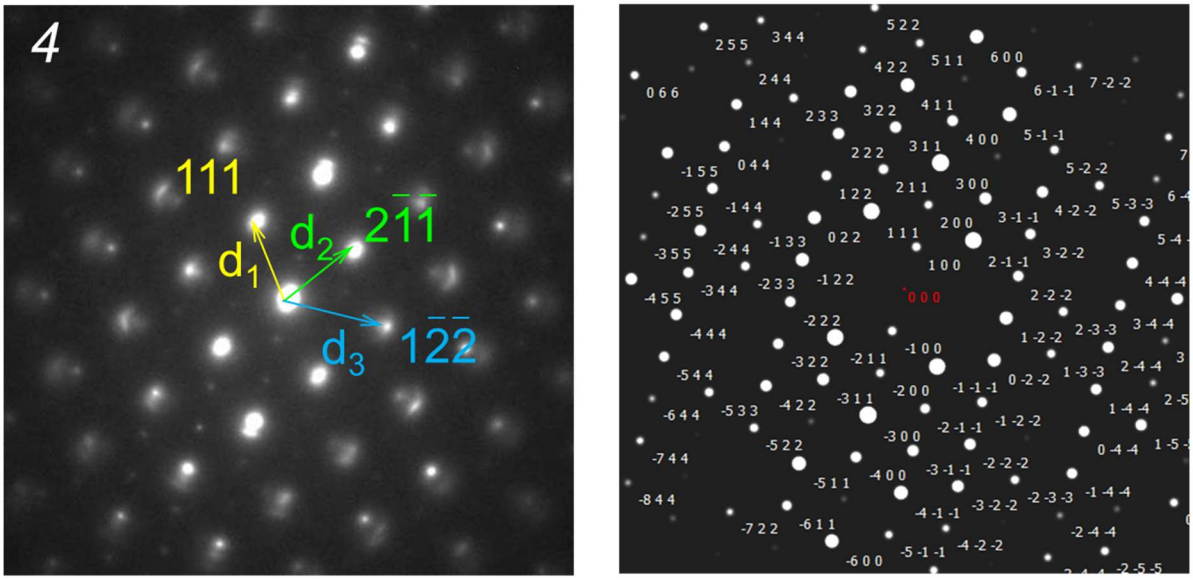

Material	LaF_3
Zone axis	[0 $\bar{1}$ 1]
Crystal system	trigonal
Space group	$P\bar{3}c1$
	a = 0.7185 nm
	c =0.7351 nm
	γ = 120 °

d-spacing			
Experimental / nm		Simulated / nm	
(d_1)	0.320	(d_{111})	0.3228
(d_2)	0.322	($d_{2\text{-}1\text{-}1}$)	0.3228
(d_3)	0.266	($d_{1\text{-}2\text{-}2}$)	0.2569

Figure S3. Experimental (upper left) and simulated (upper right) ED patterns collected from the cross section of LaF_3 half-cells with various charge states. Miller indexes are also shown in the simulated ED pattern. Italic numbers shown in experimental ED pattern indicate the analysed points or areas as shown in Figure 5 in the text. The assumed crystal structure for simulation is shown in the lower right. Three sets of d-spacing values calculated from the experimental ED pattern and determined by simulation are shown in lower left. All sets of d-spacing values were almost identical, indicating that the assumed crystal structure is true.

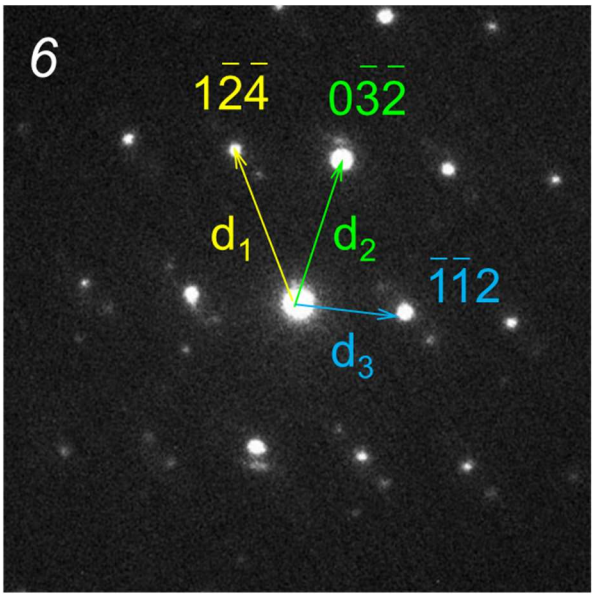

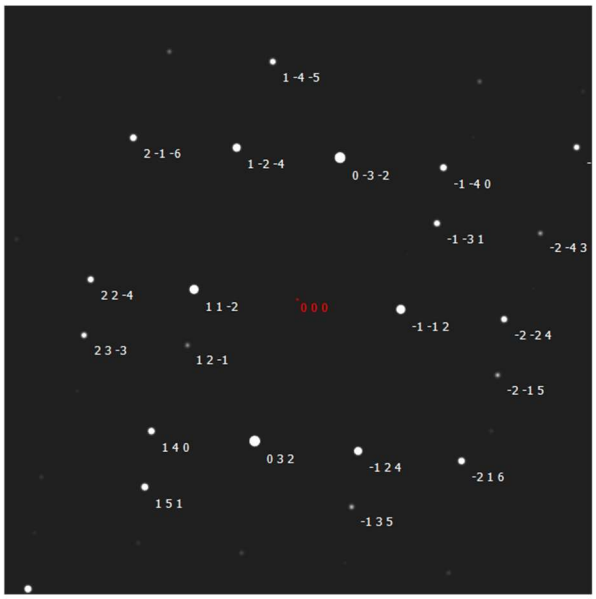

Material	LaF_3
Zone axis	[8 $\bar{2}$ 3]
Crystal system	trigonal
Space group	$P\bar{3}c1$
	a = 0.7185 nm
	c =0.7351 nm
	γ = 120 °

d-spacing	
Experimental / nm	Simulated / nm
(d_1) 0.162	($d_{1\text{-}2\text{-}4}$) 0.1636
(d_2) 0.180	($d_{0\text{-}3\text{-}2}$) 0.1806
(d_3) 0.252	($d_{\text{-}1\text{-}12}$) 0.2569

Figure S3. continued

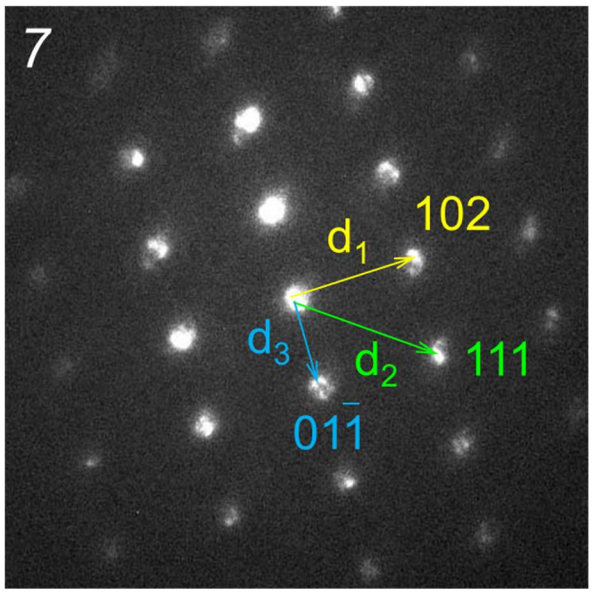

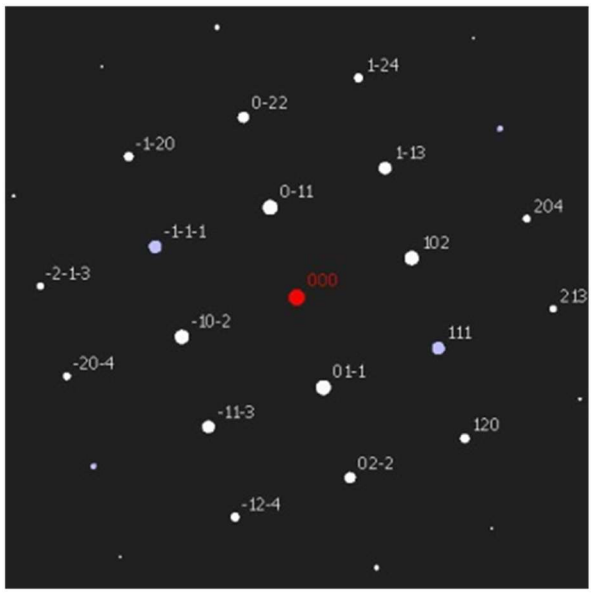

Material	La
Zone axis	$[2\ \bar{1}\ \bar{1}]$
Crystal system	hexagonal
Space group	$P6_3/mmc$
	a = 0.375nm
	c = 0.607nm
	γ *= 120 °*

d-spacing			
Experimental / nm		Simulated / nm	
(d_1)	0.222	(d_{102})	0.2218
(d_2)	0.177	(d_{111})	0.1798
(d_3)	0.289	($d_{01\text{-}1}$)	0.2870

Figure S3. continued

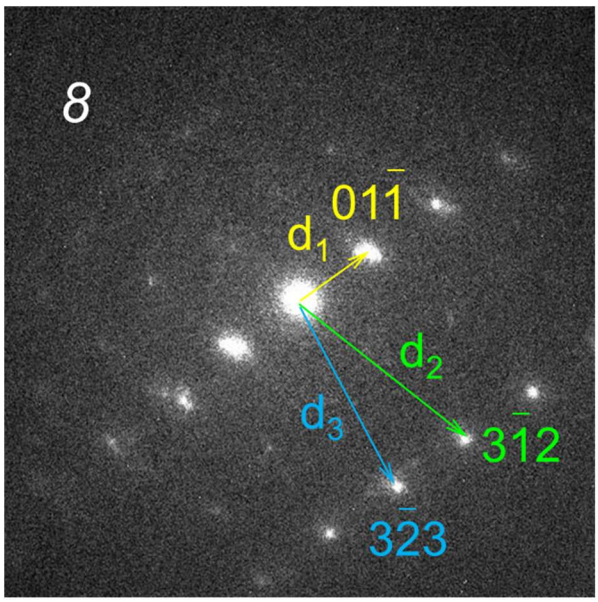

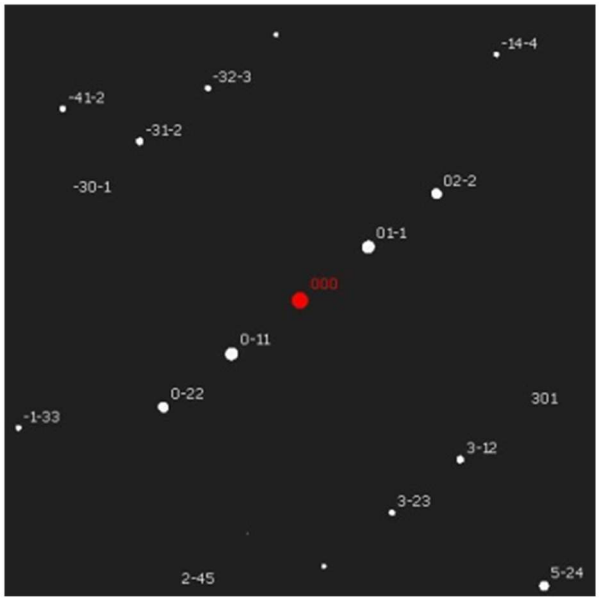

Material	La
Zone axis	$[\bar{1}\ 3\ 3]$
Crystal system	hexagonal
Space group	$P6_3/mmc$
	$a = 0.375nm$
	$c = 0.607nm$
	$\beta = 120°$

d-spacing	
Experimental / nm	Simulated / nm
(d_1) 0.318	$(d_{01\text{-}1})$ 0.31532
(d_2) 0.119	$(d_{3\text{-}12})$ 0.1181
(d_3) 0.120	$(d_{3\text{-}23})$ 0.1209

Figure S3. continued

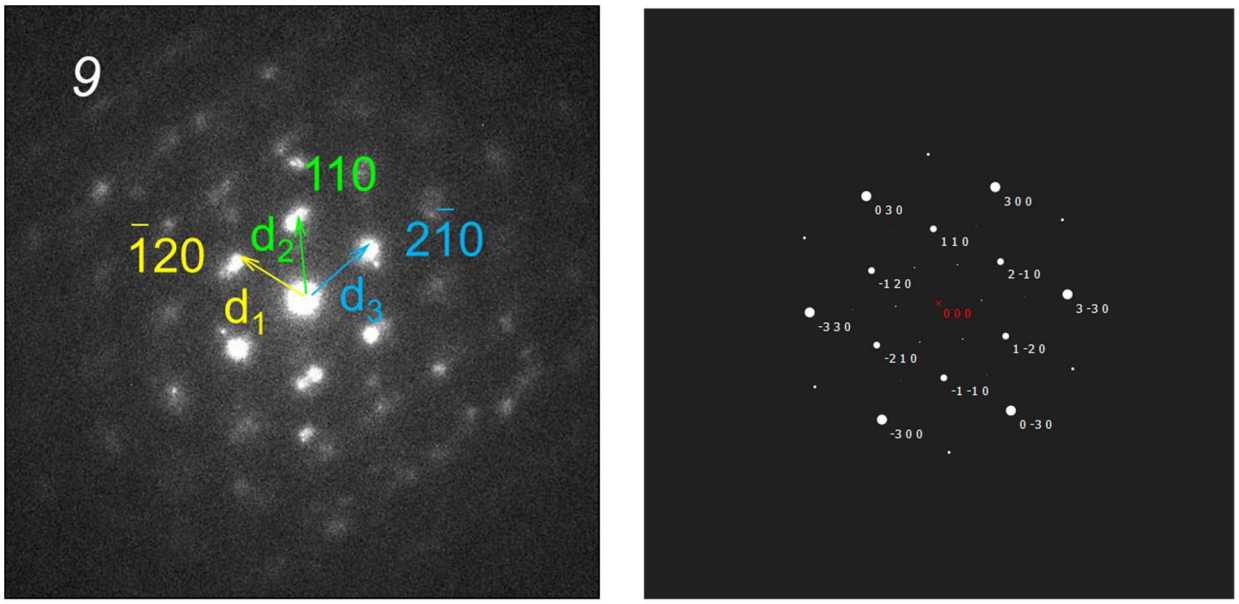

Material	LaF_3
Zone axis	[0 0 1]
Crystal system	trigonal
Space group	$P\bar{3}c1$
	a = 0.7185 nm
	c =0.7351 nm
	γ = *120 °*

d-spacing			
Experimental / nm		Simulated / nm	
(d_1)	0.355	(d_{-120})	0.3593
(d_2)	0.351	(d_{110})	0.3593
(d_3)	0.351	(d_{2-10})	0.3593

Figure S3. continued

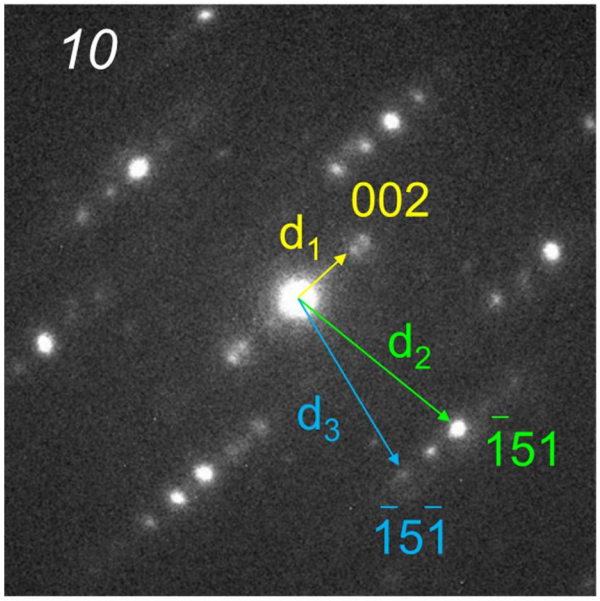

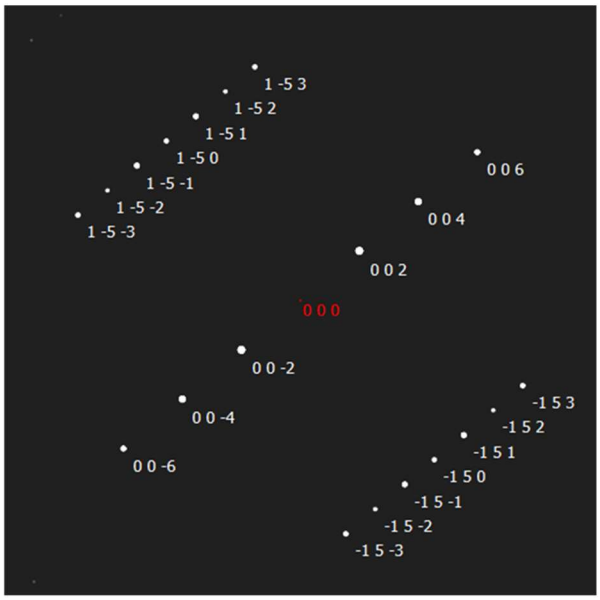

Material	LaF_3
Zone axis	[5 1 0]
Crystal system	trigonal
Space group	$P\bar{3}c1$
	a = 0.7185 nm
	c =0.7351 nm
	$\gamma = 120\,^{\circ}$

d-spacing			
Experimental / nm		Simulated / nm	
(d_1)	0.371	(d_{002})	0.36755
(d_2)	0.133	(d_{-151})	0.13352
(d_3)	0.132	(d_{-15-1})	0.13352

Figure S3. continued

Table S2. Detailed conditions for the sputtering of thin-film electrodes.

Thin film	Thickness nm	RF power W	Sputtering rate nm s^{-1}	Flow gas	pressure Pa	substrate temperature °C
Cu	2.3 or 60	50	0.033	Ar	1.0	RT
W	50	120	0.033	Ar	1.0	RT
Pt	50	50	0.025	Ar	1.0	RT
Pb	1000	50	0.025	Ar	1.0	RT
PbF_2	20	100	0.25	Ar	1.0	300